Environmental influence on phytoplankton communities in the northern Benguela ecosystem

R. Barlow[1,2,*], T. Lamont[3,2], D. Louw[4], M-J. Gibberd[2], R. Airs[5], A. van der Plas[4]

[1] *Bayworld Centre for Research and Education, Cape Town, South Africa*
[2] *Marine Research Institute & Department of Oceanography, University of Cape Town, Cape Town, South Africa*
[3] *Branch: Oceans and Coastal Research, Department of Environmental Affairs, Cape Town, South Africa*
[4] *National Marine Information and Research Centre, Swakopmund, Namibia*
[5] *Plymouth Marine Laboratory, Plymouth, United Kingdom*
** Corresponding author, e-mail: rgb.barlow@gmail.com*

ABSTRACT

An investigation of surface phytoplankton communities was undertaken on the shelf of the northern Benguela upwelling ecosystem during austral autumn (May) and spring (September) using microscopic identification and CHEMTAX analysis of pigment biomarkers on latitudinal transects at 20°S and 23°S up to 70 nautical miles offshore, and on a zigzag grid located between these transects. During May 2014, warmer, more saline water with a shallower upper mixed layer corresponding to periods of less intense offshore Ekman transport was encountered on the shelf. Satellite imagery indicated high biomass extending for a considerable distance from the coast, and CHEMTAX indicated diatoms dominating at most of the stations (52-92%), although dinoflagellates were dominant at some inshore localities (57-74%). Species of *Chaetoceros*, *Bacteriastrum* and *Cylindrotheca* were the most abundant, with *Pseudo-nitzschia* seriata-group abundance being particularly high at a number of stations. In September 2014, more intense wind forcing resulted in a deeper upper mixed layer and stronger upwelling of colder, less saline water. Elevated phytoplankton biomass was confined close to the coast where diatoms accounted for most of the population (54-87%), but small flagellates such as prasinophytes, haptophytes and cryptophytes, and the cyanobacterium *Synechococcus*, dominated the communities (58-90%) further away from the coast. It is hypothesized that stronger upwelling and deeper vertical mixing in September 2014 were not conducive for wide-spread diatom growth, and that small flagellates populated the water column by being entrained from offshore onto the shelf in the upwelled water that moved in towards the coast.

Keywords*:* Phytoplankton, Pigments, Species, Hydrography, Benguela upwelling ecosystem

Introduction

The Benguela ecosystem off southwest Africa is one of the major upwelling systems in the world's ocean and is characterised by cold nutrient-rich water and high plankton productivity on the continental shelf (Nelson and Hutchings 1983; Shannon and Nelson 1996; Hutchings et al. 2009). The northern region of the ecosystem is located off Namibia (17°-29°S) and upwelling is driven by intense along-shore southeasterly winds, facilitated by low eddy activity and a shallow mixed layer on a relatively wide shelf (Lachkar and Gruber 2012). There are seasonal fluctuations in the wind field and the climatology indicates peaks in wind stress during April-May and August-September (Louw et al. 2016). There is a consequent seasonality in upwelling and surface water temperatures, with lower surface temperatures in the period June to October and higher surface temperatures during December to May (Louw et al. 2016).

In response to changing upwelling conditions, phytoplankton biomass is highly variable on the Namibian shelf. Previous investigations by Estrada and Marrasé (1987) demonstrated patchy distributions of phytoplankton, with chlorophyll *a* levels of 20 mg m^{-3} at various localities near the coast in 15°-16°C water. Barlow et al. (2001) measured 0.3-18.5 mg m^{-3} on the shelf south of Walvis Bay in winter, with the high levels being observed at shallow stations, while chlorophyll *a* ranging from 18.4 mg m^{-3} near the coast (11°-12°C water) to 0.6 mg m^{-3} 100 km offshore (16°-17°C water) were observed during a spring

survey between 19°S and 25°S (Barlow et al. 2006). In a recent 12 year *in situ* study on a transect at 23°S in the centre of the Namibian upwelling system, Louw et al. (2016) observed that major blooms where chlorophyll *a* was >18 mg m^{-3} occurred in 5 of the 12 years and minor blooms (10-13 mg m^{-3}) were observed every year. Maxima usually developed inshore each year with peaks in April (autumn), August (winter) and December (summer). The forcing mechanisms driving these patterns are complex and include dynamic variability in wind, temperature, mixing, stratification and thermocline development, and nutrient availability. Similar changes in chlorophyll *a* occur in the upwelling ecosystem off central Chile where Anabalon et al. (2016) observed seasonal variability at a coastal site with two maxima of 8-10 mg m^{-3} in the spring (October) and summer (January). In the upwelling system off central Oregon Du et al. (2015) also noted that peaks in chlorophyll *a* of 15-20 mg m^{-3} occurred in the boreal summer months of July and August.

Phytoplankton composition of diatoms and dinoflagellates was originally identified by microscopy in the 1960's (Kollmer 1962, 1963) and by Kruger (1980), who also noted many small flagellates that were difficult to identify and quantify by microscopy. More recently community structure has also been elucidated using pigment indices and a spring survey during 2000 by Barlow et al. (2006) indicated diatoms dominating closer to the coast, while small flagellates were generally more prominent in the offshore communities. Pigments have been useful to characterize phytoplankton populations in the southern Benguela ecosystem, where fucoxanthin, peridinin and zeaxanthin are biomarkers of diatoms, dinoflagellates and cyanobacteria, respectively. 19'-Hexanoyloxyfucoxanthin (haptophytes), 19'-butanoyloxyfucoxanthin (pelagophytes), chlorophyll *b* (prasinophytes) and alloxanthin (cryptophytes) are useful biomarkers for the small flagellates (Barlow et al. 2001, 2005, Fishwick et al. 2006). Microscopy revealed that the small flagellates in the 2000 spring survey were dominated by *Emiliania huxleyi*, while a substantially calcified *E. huxleyi* morphotype was also observed inshore immediately succeeding the decline in the coastal diatom blooms (Henderiks et al. 2012).

Investigations on succession have demonstrated a transition from dinoflagellates, coccolithophores and microflagellates in newly upwelled water to diatom dominance in matured upwelled water, and a change from diatoms to dinoflagellates in aged water (Hansen et al. 2014). In a complementary study in shipboard mesocosms, it was found that diatoms dominated in newly upwelled water, but autotrophic and heterotrophic dinoflagellates were then dominant at the matured stage (Wasmund et al. 2014). Water types were originally defined for the southern Benguela ecosystem where newly upwelled water had temperatures of <10°C and nitrate concentrations of 15-30 mmol m^{-3}, matured upwelled water temperatures were 10-15°C and nitrate levels were 2-15 mmol m^{-3}, while aged water contained low concentrations of nitrate (<2 mmol m^{-3}) and temperatures of 12-16°C (Barlow 1982a). Communities were observed to be in an active phase of growth in newly upwelled and mature water but were in a slow-growing phase in aged water. A study by Louw et al. (2017) noted that the diatom genus, *Pseudo-nitzschia*, occurs frequently on the central Namibian coast and blooms developed in mature water when there was a decrease in wind stress and upwelling.

The high phytoplankton biomass off Namibia has sustained higher trophic levels and a rich marine fishery, but there has been a decline in commercial fish catches mainly due to overfishing (Finney et al. 2010). Furthermore, global climate change may have an impact on the Benguela ecosystem through atmospheric forcing (Bakun et al. 2010) and negatively affect both environmental and plankton patterns with consequent repercussions for the fragile fisheries industry. Under a warming scenario, phytoplankton composition could shift from diatom dominance to mixed communities where small flagellates and prokaryotes might contribute a greater proportion to the biomass, or perhaps become dominant under certain conditions. This would have an impact on zooplankton communities and Verheye et al (2016) report a shift from large to smaller zooplankton in the Benguela ecosystem since the mid-1990s, which in turn is likely to have an impact on higher trophic levels such as pelagic and demersal fish. The contribution of flagellates and prokaryotes to phytoplankton populations in the contemporary Namibian ecosystem is not well understood and an opportunity arose to examine community structure in more detail during two research cruises on the central shelf during May and September 2014. The approach was to

collect surface samples for phytoplankton pigments and analyse the detailed pigment data using the statistical technique of CHEMTAX (Mackey et al. 1996; Higgins et al. 2011). CHEMTAX yields information about the contribution to the total chlorophyll *a* (TChla) by the various flagellates mentioned above as well as the diatoms, dinoflagellates and prokaryotes (Higgins et al., 2011). Samples for microscopic analysis were also taken to elucidate details of the dominant diatom and dinoflagellate species. The objective was to examine the changing proportions of diatoms, dinoflagellates, flagellates and prokaryotes in surface waters at the time of the research cruises, and assess the impact of different seasonal environmental conditions on community structure.

Methods

Hydrography and sampling

The research cruises were undertaken on the Namibian shelf during 9-15 May and 8-13 September 2014 respectively. Hydrographic measurements and sampling were conducted on latitudinal transects located at 20^{o}S and 23^{o}S at 8-9 stations varying from 2-70 nm (nautical miles) from the coast (Figure 1). In addition, further measurements and sampling were conducted at stations on a zigzag grid (ZZ1-ZZ14) located between 20^{o}S and 23^{o}S (Figure 1). The water column was profiled for temperature and salinity utilizing a Seabird CTD that was maintained regularly and calibrated according to the manufacturer's instructions. Nutrient samples (50 ml) were drawn from the CTD rosette bottles at 10 m or 20 m depth intervals on the 20^{o}S and 23^{o}S transects only, filtered on board, and stored frozen for later analysis ashore using standard auto-analyser techniques (Mostert 1983). Surface seawater samples within the upper 2-5 m (200 ml) were taken for species identification only at the 20^{o}S and 23^{o}S stations and preserved with 5 ml of 40% formaldehyde (Throndsen 1978). Further surface samples were drawn for pigment analysis (1000 ml) at the 20^{o}S and 23^{o}S stations, and at the ZZ stations, and filtered through GFF filters that were stored frozen at -80^{o}C for analysis ashore. The depth of the upper mixed layer (Z_m) was determined as the depth where the local change in density was ≥0.03 kg m^{-3} using density profiles and a threshold gradient criterion (Thomson and Fine 2003).

Ekman transport at 20^{o}S and 23°S was computed from daily NCEP-DOE Reanalysis 2 meridional wind vectors according to Lamont et al. (2017). Wind vectors were rotated to account for the orientation of the coastline and wind stress was computed using the non-linear drag coefficient defined by Large and Pond (1981) and modified by Trenberth et al. (1990) for low wind speeds. Ekman transport (m^3 s^{-1} 100 m^{-1} of coastline) was then computed, with positive values indicating offshore transport (upwelling), and negative values representing onshore transport (downwelling). Daily values were summed to provide an estimate of the monthly cumulative offshore Ekman transport at 20^{o}S and 23°S. Standard monthly-averaged chlorophyll *a* data and Sea Surface Temperature (SST) from MODIS-Aqua (v2018.0), at 4.5 km spatial resolution (NASA 2018), was downloaded for May and September 2014 from the Ocean Biology Processing Group (OBGP) at NASA's Goddard Space Flight Center (GSFC; http://oceancolor.gsfc.nasa.gov). It was difficult to obtain clear enough satellite images of daily or weekly-averaged chlorophyll *a* and SST due to extensive cloud cover and fog along the Namibian coast and shelf and therefore only monthly-averaged images were found to be suitable.

Phytoplankton identification

Species identification and counts were performed with a Zeiss Axiovert 200 inverted light microscope (Utermöhl 1958). Prior to counting, formalin-preserved samples were settled in a 25 ml chamber for 24 h. Concentrations of cells were calculated using the equation of Utermöhl (1958) and counting of at least 400 cells with a precision of ±10%. Where species occurred in low concentrations, 50–200 cells were counted, providing a precision of 15–30% for quantitative estimates (Andersen and Throndsen 2004).

Pigment analysis and CHEMTAX

Pigments were extracted in 90 % acetone, aided by the use of ultrasonication, clarified by centrifugation and filtration, and analysed by HPLC (ThermoScientific Accela) using a Waters Symmetry C8 column (150 x 2.1 mm, 3.5 µm particle size, thermostated at 25^{o}C) according to Zapata et al. (2000). Pigments were detected at 440 and 660 nm and identified by retention time and on-line diode array spectra. Monovinyl chlorophyll *a* standard was obtained from Sigma-Aldrich Ltd and other pigment standards were purchased from the DHI Institute for Water and Environment, Denmark. Quality assurance protocols followed Van Heukelem and Hooker (2011). The method separates divinyl and monovinyl chlorophyll *a*, zeaxanthin and lutein, but does not resolve divinyl and monovinyl chlorophyll *b*. Limits of detection were of the order of 0.001 mg m^{-3}.

To determine community composition, pigment data was analysed by CHEMTAX (Mackey et al. 1996) following Higgins et al. (2011), with chemotaxonomic groups being identified according to Jeffrey et al. (2011). An assumption made using CHEMTAX is that the pigment:chlorophyll *a* ratios are constant across all the samples within each analysis. Therefore analysis was performed separately for each cruise such that all samples for May 2014 were run together, and then all samples for September 2014 were run together. Pigment starting ratios were obtained from Higgins et al. (2011) and Table 1 indicates the identified functional groups and the various starting and output ratios for each group. To ease the presentation of the chemotaxonomic data, diatoms-1 and -2 were combined into a collective diatom group, and prasinophytes-1 and -3 were combined into a collective prasinophyte group. Data for chlorophytes is not presented as CHEMTAX indicated that the contribution of this group was very low.

CHEMTAX outputs are the fraction of chlorophyll *a* attributed to each functional group specified in the matrix. The HPLC method separated monovinyl chlorophyll *a* allomer, monovinyl chlorophyll *a*, monovinyl chlorophyll *a* epimer and chlorophyllide *a*, and in CHEMTAX the sum of all 4 was used as the total chlorophyll *a* concentration (TChla). Chlorophyllide *a* was included as it can be generated from artificial degradation of chlorophyll *a* by chlorophyllase activity during sample handling and extraction when diatoms are present (Jeffrey and Hallegraeff 1987). The software may not discover the best global solution if it encounters local minima in the process. To circumvent this possibility, multiple starting points were used. Sixty-nine further pigment ratio tables were generated by multiplying each cell of the initial table by a randomly determined factor F, calculated as:

$$F = 1 + S \times (R - 0.5)$$

where S is a scaling factor of 0.7, and R is a random number between 0 and 1 generated using the Microsoft Excel RAND function (Wright et al., 2009). Each of the 69 ratio tables was used as the starting point for a CHEMTAX optimization. The solution with the smallest residual was used for the estimated taxonomic abundance.

Results

Hydrography

Monthly-averaged satellite images are presented to set the geographic and hydrographic context for the study area, indicating that warmer water prevailed during May 2014 compared to cooler water conditions in September 2014 (Figure 1a and c). The chlorophyll *a* image for May 2014 revealed high levels along the coast between 25^{o}S and 19^{o}S, with an offshore extension to the ZZ stations (Figure 1b). In September 2014, chlorophyll *a* was elevated inshore from Walvis Bay to Toscanini, with patchy lower concentrations between 20^{o}S and 21^{o}S (Figure 1d). Levels were much lower further offshore between 23^{o}S and 20^{o}S.

Daily offshore Ekman transport showed a decreasing trend during the cruise period in May 2014, with values decreasing from 130 m^{3} s^{-1} 100 m^{-1} on 9 May to 18 m^{3} s^{-1} 100 m^{-1} on 13 May at 20°S, increasing slightly to 55 m^{3} s^{-1} 100 m^{-1} by 15 May (Figure 2a). Similarly, Ekman transport decreased from 163 m^{3} s^{-}

^{1} 100 m^{-1} on 9 May to 11 m^3 s^{-1} 100 m^{-1} on 12 May at 23°S, then increasing to 51 m^3 s^{-1} 100 m^{-1} by 15 May (Figure 2b). In contrast, the opposite pattern was observed during the cruise in September 2014, with offshore Ekman transport increasing from 5 m^3 s^{-1} 100 m^{-1} on 8 September to 98 m^3 s^{-1} 100 m^{-1} on 10 September at 20°S, and then fluctuating between 30 and 70 m^3 s^{-1} 100 m^{-1} during 11-13 September (Figure 2c). Ekman transport also increased from 32 m^3 s^{-1} 100 m^{-1} on 8 September 2014 to 170, 138 and 142 m^3 s^{-1} 100 m^{-1} on 10, 11 and 12 September respectively at 23°S (Figure 2d). Monthly values of cumulative offshore Ekman transport at 23°S indicated that upwelling-favourable winds during September 2014 (4003 m^3 s^{-1} 100 m^{-1}) were nearly twice the intensity of that in May 2014 (2295 m^3 s^{-1} 100 m^{-1}). The difference in monthly cumulative offshore Ekman transport at 20°S was less, being 2424 m^3 s^{-1} 100 m^{-1} in September 2014 compared to 1520 m^3 s^{-1} 100 m^{-1} in May 2014, but still indicating greater offshore transport in the spring.

In situ surface temperature and salinity data indicated warmer, more saline waters at the surface on the 20°S and 23°S transects during May 2014. Along 20°S, 15-16°C water was observed inshore at the surface and 18-19°C offshore between 40 and 70 nm (Figure 3a), while at 23°S surface temperatures were 14-15°C inshore and 15-17°C offshore (Figure 3b). Surface salinities of 35.4-35.5 inshore and 35.5-35.6 offshore (40-70 nm) were noted for the 20°S transect (Figure 4a), while salinities of 35.2-35.3 prevailed across the 23°S transect in May 2014 (Figure 4b). The estimated depth of the upper mixed layer varied from 25-75 m along 20°S and was <50 m on 23°S (Figures 3, 4). Lower surface temperatures and salinities were observed in September 2014, with 12-13°C water close inshore on 20°S, 13-14°C from 2-30 nm, and 14-15°C between 30 nm and 70 nm (Figure 3c). Along 23°S, surface temperatures were 11.5-13°C inshore up to 25 nm from the coast and 13-15°C further offshore (Figure 3d). Surface salinities of 35.1-35.2 were noted from the coast to 40nm on 20°S and 35.2-35.3 beyond 40 nm (Figure 4c), while salinities of 34.9-35.0 were measured out to 50 nm on 23°S and 35.0-35.1 between 50 and 70 nm (Figure 4d). Upper mixed layers were <50 m on 20°S in September 2014, but varied from 15-100 m on 23°S (Figures 3 and 4).

Two longitudinal transects were designated for the ZZ stations, a coastal transect for the odd numbered stations, and an offshore transect for the even numbered stations (Figure 1). Surface temperatures were uniform at 14°C along the coastal transect in May 2014 (Figure 5a) and varied from 12.5-14°C in September 2014 (Figure 5c). Salinity was 35.3-35.4 in May 2014 and 35.1-35.2 in September 2014 (data not shown). The upper mixed layer on this coastal transect was 17-18 m in May 2014, but only 3 m at ZZ1, and varied between 5 m and 30 m in September 2014 (Figure 5a, c). Surface temperatures were higher along the offshore ZZ transect, being 16-17°C in May 2014 (Figure 5b) and 14-15°C in September 2014 (Figure 5d). Surface salinity varied from 35.3-35.5 in May 2014 and was lower in September 2014 at 35.0-35.2 (data not shown). Mixed layer depths on the offshore ZZ transect were <50 m during both May and September 2014 (Figure 5b, d).

Phytoplankton species

Only the dominant species of diatoms and dinoflagellates on the 20°S and 23°S transects are listed in Table 2 as a more detailed account of all species will be reported elsewhere. The criterion for dominance was selected as the highest abundance for 1-3 species at each station compared to other species that had lower abundances. Dominant cell counts varied widely, however, and examples are the 30 nm station on 20°S in May 2014 where abundance was 1.39-2.67 x 10^6 cells L^{-1}, while at the 50 nm station on 23°S, cell counts were 1.05-1.14 x 10^3 cells L^{-1} (Table 2).

Diatoms were dominated by various species on each transect and the *Pseudo-nitzschia* seriata-group, *Chaetoceros curvisetus* and *Chaetoceros debilis* were the most abundant up to 30 nm on 20°S during May 2014. *Thalassiosira gravida*, *Bacteriastrum delicatulum*, *Bacteriastrum hyalinum*, *Cylindrotheca closterium*, *Pseudo-nitzschia* seriata-group, *Rhizosolenia robusta* and a *Thalassiosira* sp were the dominant diatoms from 40-70 nm, with the particular details for each station presented in Table 2. These species were also the dominant diatoms on 23°S in May 2014 and the *Pseudo-nitzschia* seriata-group was

particularly dominant at six of the nine stations (Table 2). The dominant dinoflagellates on the 20°S transect included *Ceratium* spp., *Prorocentrum micans*, *Corythodinium tesselatus*, *Gyrodinium* spp., *Protoperidinium pallidum* and *Protoperidinium* spp., although unidentified dinoflagellates were also present at some of the stations. For 23°S, *Prorocentrum micans, Protoperidinium* spp. and *Scrippsiella trochoidea* were the dominant species, but the abundance of naked dinoflagellates and unidentified dinoflagellates appeared to be greater on this transect (Table 2).

A change in diatom species was observed in September 2014 where the dominant species on 20°S were *Thalassiosira gravida*, *Pseudo-nitzschia* seriata-group, *Thalassiosira rotula*, *Leptocylindrus danicus*, *Thalassiosira anguste-lineata*, *Chaetoceros decipiens* and *Chaetoceros didymus*, with varying abundances between stations (Table 2). Different species were generally dominant on 23°S that included *Skeletonema japonica*, *Navicula* spp., *Pseudo-nitzschia* delicatissima-group, *Chaetoceros curvisetus*, *Chaetoceros constrictus*, *Chaetoceros convolutes*, *Chaetoceros atlanticus* and *Pseudo-nitzschia* seriata-group (Table 2). There was also a general change in dinoflagellates for September 2014 and *Gyrodinium* spp., *Gymnodenium* spp., *Protoperidinium* spp., *Scrippsiella trochoidea*, *Noctiluca scintillans*, *Ceratium furca*, *Dinophysis fortii*, *Prorocentrum triestinum* and *Dinophysis acuminate* were the dominant species on 20°S. Four of these dinoflagellates were also dominant on 23°S in addition to *Prorocentrum triestinum* and *Protoperidinium oblongum* (Table 2). Unidentified dinoflagellates were also present in significant numbers at some stations on both the 20°S and 23°S transects.

CHEMTAX

The pattern of community structure as determined by CHEMTAX is presented together with surface temperature and nutrient data in Figures 6 to 9. Surface temperatures on the 20°S transect were 15°-18°C in May 2014 compared to 13°-14.5°C in September 2014 and there was a general decrease in the concentrations of nitrates and silicates from inshore to offshore, although they did not appear to reach limiting levels of <1 mmol m^{-3} (Barlow et al. 2006) as all concentrations were >2 mmol m^{-3} (Figure 6a, d). TChla concentrations ranged from 1.1-3.4 mg m^{-3} in May 2014, but was more variable in September 2014 where TChla was 2.2-8.0 mg m^{-3} at inshore stations and 0.8-2.6 mg m^{-3} between 10 and 70 nm offshore (Figure 6b, e). Phytoplankton communities in May 2014 were dominated by dinoflagellates at the 2, 10 and 20 nm stations (57-74%) and by diatoms at the 30-70 nm stations (71-92%), with the small flagellate (haptophytes, pelagophytes, cryptophytes, prasinophytes) and prokaryote (*Synechococcus*) groups contributing <20% (Figure 6c). The diatom proportion was 45-88% at the 2-60 nm stations in September 2014, but the flagellate contribution was 76% at the 70 nm station, with prasinophytes accounting for at least half (Figure 6f).

On the 23°S transect, surface temperatures were also higher in May 2014 (14°-16.5°C) than September 2014 (12°-14.5°C), with highly variable nitrate and silicate concentrations that were >2 mmol m^{-3} (Figure 7a, d). TChla levels were 1.2-2.4 mg m^{-3} across the transect in May 2014 and 0.8-2.2 mg m^{-3} in September 2014 (Figure 7b, e). Diatoms dominated the populations on the transect in May 2014 (47-78%), although dinoflagellates and pelagophytes contributed 24% and 21% respectively at the 2 nm station and dinoflagellates 29% at 30 nm (Figure 7c). Flagellates were dominant in September 2014 (56-100%) although diatoms were 55% at the 20 nm station (Figure 7f). Prasinophytes accounted for most of the flagellates at the 2-50 nm stations, *Synechococcus* contributed 42% and 30% at 40 nm and 50 nm, while haptophytes contributed 32% at the 70 nm station.

No nutrient data was available for the ZZ stations but surface temperatures were 13.9°-14.7°C at the inshore ZZ stations in May and 12.4°-13.7°C in September 2014 (Figure 8a, d). The highest TChla levels were observed at the southern ZZ1 station in both May (4.5 mg m^{-3}) and September 2014 (7.7 mg m^{-3}), with lower TChla at the other inshore ZZ stations (Figure 8b, e). Dinoflagellates were generally the dominant phytoplankton group (47-70%) in May 2014 (Figure 8e), but in September 2014 the diatoms were mostly dominant (33-73%) together with some of the flagellates (Figure 8f). Prasinophytes

contributed 28-45% at the ZZ1, 3, 5 and 7 stations, and cryptophyes were 19-32% at the ZZ 11 and 13 stations (Figure 8f).

Temperatures at the offshore ZZ stations were higher in May (16.0^{o}-17.0^{o}C) compared to September 2014 (14.2^{o}-15.2^{o}C) (Figure 9a, d), and overall surface waters at these offshore stations were also warmer than at the inshore stations during both months. TChla at these offshore stations was 1.2-10.2 mg m^{-3} in May 2014 but lower in September (0.7-1.5 mg m^{-3}; Figure 9b, e). Diatoms dominated 52-92% at all stations in May 2014 (Figure 9e) but the flagellates were collectively more dominant (59-97%) in September 2014 (Figure 9f). While the diatoms were dominant at ZZ2 (57%), the haptophytes and prasinophytes contributed 13-50% and 12-44% respectively at the other offshore stations, and the *Synechococcus* proportion was 9-23% at some of these stations (Figure 9f).

Discussion

Previous studies in the southern Benguela ecosystem identified three stages in the evolution of upwelled water, namely newly upwelled water, matured water and aged water (Barlow 1982a, 1982b; Brown and Hutchings 1987). More recently, in a study of phytoplankton succession in the northern Benguela, Hansen et al. (2014) developed more suitable hydrographic criteria for these stages for the northern Benguela. Applying the criteria of Hansen et al. (2014) to the current data indicated that the water masses in May 2014 were in a late mature to aged stage on the 20^{o}S, 23^{o}S and ZZ transects. This is in agreement with the offshore Ekman transport that exhibited a decreasing pattern during the May cruise period, and implied that the sampling was conducted during the declining phase of an upwelling event. During September 2014, the Hansen et al. (2014) criteria suggested that the water was in a newly upwelled stage, with a tendency towards the mature stage at the outer three stations on 20^{o}S and 23^{o}S. This corresponded well with the offshore Ekman transport that displayed an increasing pattern during the cruise period in September, implying that sampling took place during the early phase of an upwelling event.

Hansen et al. (2014) observed diatom dominance in matured upwelled water, with a decline in diatoms and a succession to domination by dinoflagellates in the later stage of aged water. The CHEMTAX analysis of pigment data in this study indicated that diatoms were also dominant in aged water at most of the stations during May 2014, although dinoflagellates were dominant at the three inshore stations on 20^{o}S and at the inshore ZZ stations (Figures 6 and 8). Mixed populations of nanoflagellates, coccolithophores and dinoflagellates were observed in newly upwelled water by Hansen et al. (2014). Similarly, small flagellates tended to be dominant in the newly upwelled water during September 2014, although diatoms and dinoflagellates were present in lower proportions. Prasinophytes and haptophytes contributed the greater proportion of the nanoflagellate component, and there was also a substantial proportion of the prokaryote *Synechococcus* (Figures 7 and 9). Thus, even though this investigation could only provide a "snapshot" of two stages of upwelling, there are similarities between the results of Hansen et al. (2014) for August-September 2011 and the observations here for May and September 2014. Although only surface characteristics are reported, Barlow et al. (2006) demonstrated that these communities are representative of the population within the water column for stations closer to the coast, but for stations towards the shelf edge the dominance of small flagellates in the upper mixed layer usually decreased at deeper depths where diatoms tended to be more dominant.

While CHEMTAX analysis was useful for indicating change in the bulk proportion of phytoplankton groups, microscopy provided details about the differences in species of diatoms and dinoflagellates between the two periods of investigation. The dinoflagellates in May 2014 were mostly unidentified species that included naked dinoflagellates, but more identifiable species were observed in September 2014. For the diatoms, species of *Chaetoceros*, *Bacteriastrum* and *Cylindrotheca* were dominant during May 2014, with *Pseudo-nitzschia* seriata-group abundance being particularly high at a number of stations on the 20^{o}S and 23^{o}S transects (Table 2). In contrast, dominant diatoms in September 2014 included species of *Thalassiosira* and *Leptocylindrus*, with *Chaetoceros* and *Pseudo-nitzschia* species at a few stations. Hansen et al. (2014) also noted that *Pseudo-nitzschia* seriata-group was abundant in mature

upwelled water, together with species of *Chaetoceros* and *Thalassiosira*, but dinoflagellates of the order Gymnodiniales were dominant in aged water. Interestingly, small phytoplankton characterized the inshore newly upwelled water in August-September 2011 where *Emiliania huxleyi* and species of *Phaeocystis*, *Pyramimonas* and *Pseudopedinella* contributed a high percentage (Hansen et al. 2014). The prevalence of *Pseudo-nitzschia* species in Namibian waters (Kollmer 1963; Kruger 1980; Hansen et al. 2014) is of concern because they can be toxic to higher trophic levels. A 14 year study on the 23^{o}S transect revealed blooms of *Pseudo-nitzschia* occurring in 13-16^{o}C water, with the climatology showing an increase during austral summer, while a maximum can be attained during May-July (Louw et al. 2017). *Pseudo-nitzschia* blooms occurred during periods of low wind stress and weak upwelling (Louw et al. 2017), complementing the observations in this study where high *Pseudo-nitzschia* cell counts were observed under conditions of decreasing Ekman transport in May 2014.

This investigation indicated that small phytoplankton groups were more prominent on the Namibian shelf in September 2014 than in May 2014, particularly the prasinophytes, haptophytes and *Synechococcus* (Figures 6-9). Colder, lower salinity, nutrient sufficient water prevailed in September 2014 that was characterized as being in the first stage of newly upwelled water. Under these environmental conditions, it might be expected that diatoms would dominate as observed by Barlow (1982b) and Brown and Hutchings (1987) in the southern Benguela. However, these early studies did not evaluate the contribution of small phytoplankton cells as has been done for the northern Benguela by Hansen et al. (2014). CHEMTAX showed that although diatoms accounted for a greater proportion of the biomass on the 20^{o}S transect and at the ZZ inshore stations in September 2014, this was not the case for the 23^{o}S transect and the ZZ offshore stations (Figures 7 and 9). High phytoplankton biomass was confined much closer to the coast in September 2014 and there were patches of elevated chlorophyll *a* in the vicinity of 20^{o}S (Figure 1d). But TChla was lower on the 23^{o}S transect and at the offshore ZZ stations (Figures 1d, 7 and 9) and the flagellate groups were more dominant. The upper mixed layer was deeper on the 23^{o}S transect and at the offshore ZZ stations (Figures 3d, 4d, 5d), indicating stronger vertical mixing, driven by stronger wind conditions in September 2014 (Figure 2d). Diatoms tend to flourish and bloom when the upper mixed layer is shallow and the water column is more stratified during periods of lower wind stress and reduced Ekman transport as in May 2014 (Figures 2b, 3b, 4b, 5b), resulting in elevated phytoplankton biomass that can extend for a considerable distance offshore, as illustrated in Figure 1b.

Prominent contribution by small flagellates to phytoplankton biomass in upwelling systems is not unusual and could be considered a general feature. Crespo et al. (2011) estimated that nanoflagellates accounted for 62-80% of the integrated biomass in both coastal and oceanic domains off northwest Iberia during a spring upwelling event. A similar pattern has also been observed in the Humboldt upwelling system off northern Chile where Iriarte et al. (2000) observed that nano- and picophytoplankton contributed 80% to primary production and 63% to TChla in summer, and 67% to both in the winter. A 2 year temporal study at a coastal site in central Chile by Bottjer and Morales (2007) demonstrated that nanoflagellates were the dominant component of the phytoplankton community during all seasons, contributing up to 80% to the autotrophic biomass in the upper 50 m during both upwelling and downwelling periods. In comparison, the average proportion of flagellates (including *Synechococcus*) along the 20^{o}S transect off Namibia increased from 13% in May to 28% in September 2014, while the average proportion on the 23^{o}S transect was 27% in the May and 72% during the September cruise. The average proportion for the ZZ inshore stations increased from 23% in May to 42% in September 2014, with the average at the ZZ offshore stations being 16% and 74% in the May and September respectively. It appears therefore that small flagellates contribute substantially to phytoplankton biomass on the central shelf of Namibia, as reported for the other upwelling ecosystems.

Overall, there are important differences in physical, geochemical and biological processes between the upwelling ecosystems of the southern Pacific and southern Atlantic eastern ocean margins (3^{o}-40^{o}S) (Mackas et al. 2006). There is strong ENSO activity in the Pacific, while “Benguela Ninos” occur with decadal frequency in the Atlantic. In addition, strong coastal trapped waves are a feature in both ecosystems, although this occurs intra-seasonally in the Pacific. While hypoxia, oxygen minimum layers

and denitrification are a feature of the Pacific margin, there is a mismatch of time scales between phyto-, zoo- and meroplankton in the Atlantic margin. Trophic efficiency is higher in the southeastern Pacific, leading to greater fish production, but in contrast fish yield is lower in the southeastern Atlantic (Mackas et al. 2006).

Previously, small flagellates were observed to be more dominant at the Namibian shelf edge and on the slope (Barlow et al. 2006) and it is hypothesized that these flagellates were entrained in the upwelled water that moved inshore and up the shelf towards the coast in September 2014. The water column was not sufficiently stratified at the time of sampling for diatoms to have proliferated, and therefore the small flagellates that had populated the water column were observed to be more dominant on the 23^{o}S transect and at the offshore ZZ stations. Barange and Pillar (1992) proposed a conceptual model of cross-shelf circulation during active and quiescent phases of upwelling, and suggested that during active upwelling, shelf circulation is characterised by seaward transport of surface waters, but the flow at depth is onshore, following isopycnal surfaces. Such a transport mechanism would account for the mid-shelf observation of flagellate communities, which are more common in the offshore regions. With the stronger vertical mixing in September 2014, it is likely that flagellate communities were mixed down to a depth where they were entrained in the onshore flow. Evidence of this transport mechanism can be seen in the vertical salinity distribution along 23°S, where higher salinity water occurring at the surface between 60 and 70 nm from the coast appears to be subducted and advected shoreward below the upper mixed layer (Figure 4).

The prominence of small flagellates in contemporary upwelling ecosystems raises questions about their future role in the marine food web. The food chain in the Benguela ecosystem has been considered to be relatively simple, with mesozooplankton grazing on larger diatoms and dinoflagellates, macrozooplankton grazing on phytoplankton and mesozooplankton, small pelagic fish (anchovies, sardines) consuming predominately zooplankton, and larger fish such as hake feeding on small fish (Jarre-Teichmann et al. 1998; Hutchings et al. 2009). Besides the observation in this study, nanoflagellates have also been observed to be prominent in the southern Benguela ecosystem, predominantly offshore on the continental slope, but also on the shelf together with diatoms (Mitchell-Innes and Winter 1987; Barlow et al. 2005; Lamont et al. 2014). This implies that microzooplankton grazing probably plays an important role in the food web, grazing on the nanoflagellates and in turn being grazed by the mesozooplankton (Jarre-Teichmann et al. 1998). Thus the food web in the Benguela ecosystem is probably more complex than previously thought since this microbial loop most likely plays an important role. If there is a decline in upwelling-favourable winds due to climate change (Bakun et al. 2010), then it is likely that offshore Ekman transport would decrease along the Namibian shelf, as well as along the west coast of South Africa, leading to less or no upwelling of nutrient-rich water into the euphotic zone, with a consequent low abundance of diatoms and the dominance of nano- and picophytoplankton. The overall phytoplankton production and biomass are then likely to be lower than contemporary levels and the microbial loop would then become a key component of the food web. Meso- and macrozooplankton production and biomass could also decrease, with a resulting synergetic effect of upwelling changes and the role of the microbial loop over the biomass of small pelagic fish and larger demersal species such as hake.

Indeed, a substantial decrease in upwelling-favourable winds in the Northern Benguela has been observed in recent years (Lamont et al., 2017), and this corresponds to positive linear sea surface temperature trends suggestive of warming (Jarre et al., 2015). However, the impact of this longer-term reduction in upwelling and warming of surface waters has not yet been clearly discerned as satellite records of surface chlorophyll *a* show a seemingly contradictory trend, with higher values in recent years (Jarre et al., 2015), while zooplankton trends are in agreement with a warming scenario and show an overall decrease in abundance and a shift in dominance by smaller species (Verheye et al., 2016). Modifications in the food web structure will have important implications for the commercial fisheries of Namibia and South Africa, and therefore current ecosystem- and fisheries-based management in each country needs to be reviewed

and adjusted accordingly in consideration of the possible changes in water properties and plankton interactions.

Acknowledgements - We sincerely thank the officers and crew of the RV *Mirabilis* for their skilled cooperation and assistance during the cruise; technical staff of the Environmental sub-division at NatMIRC for shipboard and laboratory support; R Roman for nutrient analysis; the South African National Research Foundation and the National Commission on Research, Science and Technology of Namibia for funding support.

References

Anabalón V, Morales C, González H, Menschel E, Schneider W, Hormazabal S, Valencia L, Escribano R. 2016. Micro-phytoplankton community structure in the coastal upwelling zone off Concepción (central Chile): Annual and inter-annual fluctuations in a highly dynamic environment. *Progress in Oceanography* 149: 174-188.

Andersen P, Throndsen J. 2004. Estimating cell numbers. In: Hallegraeff G, Anderson D, Cembella A (eds), *Manual on Harmful Marine Microalgae*. UNESCO. pp. 99-129.

Bakun A, Field D, Redondo-Rodriguez A, Weeks S. 2010. Greenhouse gas, upwelling-favorable winds, and the future of coastal ocean upwelling ecosystems. *Global Change Biology* 16: 1213-1228.

Barange M, Pillar S. 1992. Cross-shelf circulation, zonation and maintenance mechanisms of *Nyctiphanes capensis* and *Euphausia hanseni* (Euphausiacea) in the northern Benguela upwelling system. *Continental Shelf Research* 12: 1027-1042.

Barlow R. 1982a. Phytoplankton ecology in the Southern Benguela current. I. Biochemical composition. *Journal of Experimental Marine Biology and Ecology* 63: 209-227.

Barlow R. 1982b. Phytoplankton ecology in the Southern Benguela Current. III.Dynamics of a bloom. *Journal of Experimental Marine Biology and Ecology* 63: 239-248.

Barlow R, Aiken J, Sessions H, Lavender S, Mantel J. 2001. Phytoplankton pigment, absorption and ocean colour characteristics in the southern Benguela ecosystem. *South African Journal of Science* 97: 230–238.

Barlow R, Louw D, Balarin M, Alheit J. 2006. Pigment signatures of phytoplankton composition in the northern Benguela ecosystem during spring. *African Journal of Marine Science* 28: 479-491.

Barlow R, Sessions H, Balarin M, Weeks S, Whittle C, Hutchings L. 2005. Seasonal variation in phytoplankton in the southern Benguela: pigment indices and ocean colour. *African Journal of Marine Science* 27: 275–287.

Bottjer D. Morales C. 2007. Nanoplanktonic assemblages in the upwelling area off Concepcion (~36^{o}S), central Chile: Abundance, biomass, and grazing potential during the annual cycle. *Progress in Oceanography* 75: 415-434.

Brown P, Hutchings L. 1987. The development and decline of phytoplankton blooms in the southern Benguela upwelling system. 1. Drogue movements, hydrography and bloom development. In: Payne A, Gulland J, Brink K (eds), *The Benguela and Comparable Ecosystems. South African Journal of Marine Science* 5: 357-391.

528 Crespo B, Espinoza-Gonzalez O, Teixeira I, Castro C, Figueiras F. 2011. Possible mixotrophy of
529 pigmented nanoflagellates: Microbial plankton biomass, primary production and phytoplankton growth in
530 the NW Iberian upwelling in spring. *Estuarine, Coastal and Shelf Science* 94: 172-181.
531
532 Du X, Peterson W, O'Higgins L. 2015. Interannual variations in phytoplankton community structure in
533 the northern California Current during the upwelling seasons of 2001-2010. *Marine Ecology Progress*
534 *Series* 519: 75-87.
535
536 Estrada M, Marrasé C. 1987. Phytoplankton biomass and productivity off the Namibian coast. In: Payne
537 A, Gulland J, Brink K (eds), *The Benguela and Comparable Ecosystems. South African Journal of*
538 *Marine Science* 5: 347-356.
539
540 Finney B, Alheit J, Erneis K, Field D, Gutierrez D, Struck U. 2010. Paleoecological studies on variability
541 in marine fish populations: a longterm perspective on the impacts of climatic change on marine
542 ecosystems. *Journal of Marine Systems* 79: 316-326.
543
544 Fishwick J, Aiken J, Barlow R, Sessions H, Bernard S, Ras J. 2006. Functional relationships and bio-
545 optical properties derived from phytoplankton pigments, optical and photosynthetic parameters; a case
546 study of the Benguela ecosystem. *Journal of the Marine Biological Association of the United Kingdom*
547 86: 1267–1280.
548
549 Hansen A, Ohde T, Wasmund N. 2014. Succession of micro- and nanoplankton groups in ageing
550 upwelled waters off Namibia. *Journal of Marine Systems* 140: 130–137.
551
552 Henderiks J, Winter A, Elbrächter M, Feistel R, van der Plas A, Nausch G, Barlow R. 2012.
553 Environmental controls on *Emiliania huxleyi* morphotypes in the Benguela coastal upwelling system (SE
554 Atlantic). *Marine Ecology Progress Series* 448: 51-66.
555
556 Higgins H, Wright S, Schluter L. 2011. Quantitative interpretation of chemotaxonomic pigment data. In:
557 Roy S, Llewellyn C, Egeland E, Johnsen G (eds), *Phytoplankton pigments: characterization,*
558 *chemotaxonomy and applications in oceanography*. Cambridge: Cambridge University Press. pp 257-
559 313.
560
561 Hutchings L, van der Lingen C, Shannon L, Crawford R, Verheye H, Bartholomae C, van der Plas A,
562 Louw D, Kreiner A, Ostrowski M, Fidel Q, Barlow R, Lamont T, Coetzee J, Shillington F, Veitch J,
563 Currie J, Monteiro P, 2009. The Benguela Current: an ecosystem of four components. *Progress in*
564 *Oceanography* 83: 15-32.
565
566 Iriarte J, Pizarro G, Troncoso V, Sobarzo M. 2000. Primary production and biomass of size-fractionated
567 phytoplankton off Antofagasta, Chile (23–24^{o}S) during pre-El Nino and El Nino 1997. *Journal of Marine*
568 *Systems* 26: 37-51.
569
570 Jarre A, Hutchings L, Kirkman S, Kreiner A, Tchipalanga P, Kainge P, Uanivi U, van der Plas A, Blamey
571 L, Coetzee J, Lamont T, Samaai T, Verheye H, Yemane D, Axelsen B, Ostrowski M, Stenevik E, Loeng
572 H. 2015. Synthesis: climate effects on biodiversity, abundance and distribution of marine organisms in
573 the Benguela. *Fisheries Oceanography* 24 (S1): 122-149.
574
575 Jarre-Teichmann A, Shannon L, Moloney C, Wickens P. 1998. Comparing trophic flows in the southern
576 Benuela to those in other upwelling ecosystems. *South African Journal of Marine Science* 19: 391-414.
577
578 Jeffrey S, Hallegraeff G. 1987. Chlorophyllase distribution in ten classes of phytoplankton : a problem for
579 chlorophyll analysis. *Marine Ecology Progress Series* 35: 293-304.
580

Jeffrey S, Wright S, Zapata M. 2011. Microalgal classes and their signature pigments. In: Roy S, Llewellyn C, Egeland E, Johnsen G (eds), *Phytoplankton pigments: characterization, chemotaxonomy and applications in oceanography*. Cambridge: Cambridge University Press. pp 3-77.

Kollmer W. 1962. The annual cycle of phytoplankton in the waters off Walvis Bay 1958. *Investigational Report* No. 4. South West Africa: Marine Research Laboratory. 44 pp.

Kollmer W. 1963. The pilchard of South West Africa. Monthly recordings of phytoplankton species in the area off Walvis Bay during 1959 and 1960. *Investigational Report* No. 8. South West Africa: Marine Research Laboratory. pp. 35–78.

Kruger I. 1980. A checklist of South West African marine phytoplankton, with some phytogeographical relations. *Fisheries Bulletin of South Africa* 13: 31-40.

Lamont T, Barlow R, Kyewalyanga M. 2014. Physical drivers of phytoplankton production in the southern Benguela upwelling system. *Deep-Sea Research I* 90: 1-16.

Lamont T, García-Reyes M, Bograd SJ, van der Lingen CD, Sydeman WJ. 2017. Upwelling indices for comparative ecosystem studies: Variability in the Benguela Upwelling System. *Journal of Marine Systems* (in press, http://dx.doi.org/10.1016/j.jmarsys.2017.05.007).

Lachkar Z, Gruber N. 2012. A comparative study of biological production in eastern boundary upwelling systems using an artificial neural network. *Biogeosciences* 9: 293-308.

Large W, Pond S. 1981. Open ocean momentum flux measurements in moderate to strong winds. *Journal of Physical Oceanography* 11: 324-336.

Louw D, Doucette G, Voges E. 2017. Annual patterns, distribution and long-term trends of *Pseudo-nitzschia* species in the northern Benguela upwelling system. *Journal of Plankton Research* 39: 35-47.

Louw D, van der Plas A, Mohrholz V, Wasmund N, Junker T, Eggert A. 2016. Seasonal and inter-annual phytoplankton dynamics and forcing mechanisms in the northern Benguela upwelling system. *Journal of Marine Systems* 157: 124-134.

Mackas D, Strub P, Thomas A, Montecino V. 2006. Eastern ocean boundaries pan-regional overview. In: Robinson A, Brink K (eds), The sea. The global coastal ocean: interdisciplinary regional studies and syntheses. Vol 14, part A. Cambridge MA: Harvard University Press. pp 21-59.

Mackey M, Mackey D, Higgins H, Wright S. 1996. CHEMTAX - a program for estimating class abundances from chemical markers: application to HPLC measurements of phytoplankton. *Marine Ecology Progress Series* 144: 265–283.

Mitchell-Innes B, Winter D. 1987. Coccolithophores: a major phytoplankton component in mature upwelled waters off the Cape Peninsula, South Africa in March, 1983. Marine Biology 95: 25–30.

Mostert S. 1983. Procedures used in South Africa for the automatic photometric determination of micronutrients in seawater. *South African Journal of Marine Science* 1: 189-198.

NASA Goddard Space Flight Center, Ocean Ecology Laboratory, Ocean Biology Processing Group (OBGP). 2018. Moderate-resolution Imaging Spectroradiometer (MODIS) Aqua Chlorophyll Data; 2018 Reprocessing. NASA OB.DAAC, Greenbelt, MB, USA (Accessed on 07/03/2018), doi: 10.5067/AQUA/MODIS/L3M/CHL/2018.

Nelson G, Hutchings L. 1983. The Benguela upwelling area. *Progress in Oceanography* 12: 333–356.

Shannon L, Nelson G. 1996. The Benguela: large scale features and processes and system variability. In: Wefer G, Berger W, Siedler G, Webb D (eds), *The South Atlantic: present and past circulation.* Berlin: Springer. pp 163-210.

Thomson R, Fine I. 2003. Estimating mixed layer depth from oceanic profile data. *Journal of Atmospheric and Oceanic Technology* 20: 319-329.

Throndsen J. 1978. Preservation and storage. In: Sournia A (ed), *Phytoplankton Manual*. UNESCO Monographs on Oceanographic Methodology. pp 337.

Trenberth K, Large W, Olson J. 1990. The mean annual cycle in global ocean wind stress. *Journal of Physical Oceanography* 20:1742-1760.

Utermöhl H. 1958. Zur Vervollkommnung der quantitativen Phytoplankton-Methodik. *Mitteilungen der Internationalen Vereiniung für Limnologie* 9: 1–38.

Van Heukelem L, Hooker S. 2011. The importance of a quality assurance plan for method validation and minimizing uncertainties in the HPLC analysis of phytoplankton pigments. In: Roy S, Llewellyn C, Egeland E, Johnsen G (eds), *Phytoplankton pigments: characterization, chemotaxonomy and applications in oceanography*. Cambridge: Cambridge University Press. pp 195-242.

Verheye H, Lamont T, Huggett J, Kreiner A, Hampton I. 2016. Plankton productivity of the Benguela Current Large Marine Ecosystem (BCLME). *Environmental Development* 17: 75-92.

Wasmund N, Nausch G, Hansen A. 2014. Phytoplankton succession in an isolated upwelled Benguela water body in relation to different initial nutrient conditions. *Journal of Marine Systems* 140: 163-174.

Wright S, Ishikawa A, Marchant H, Davidson A, van den Enden R, Nash G. 2009. Composition and significance of picophytoplankton in Antarctic waters. *Polar Biology* 32: 797-808.

Zapata M, Rodríguez F, Garrido J. 2000. Separation of chlorophylls and carotenoids from marine phytoplankton: a new HPLC method using a reversed phase C8 column and pyridine containing mobile phases. *Marine Ecology Progress Series* 195: 29-45.

670

Table 1

Pigment:chlorophyll *a* starting and output ratios for the CHEMTAX analysis of HPLC pigments. Starting ratios derived from Higgins et al. (2011). Chla-chlorophyll *a*; Chlb-chlorophyll *b*; MgDVP-Mg-2,4-dininyl pheoporphyrin a_5 monomethyl ester; Chlc1-chlorophyll c_1; Chlc2-chlorophyll c_2; Chlc3-chlorophyll c_3; Per-peridinin; But-19'-butanoyloxyfucoxanthin; Fuc-fucoxanthin; Neo-neoxanthin; Viol-violaxanthin; Pras-prasinoxanthin; Hex-19'-hexanoyloxyfucoxanthin; Allo-alloxanthin; Zea-zeaxanthin; Anth-antheraxanthin; Asta-astaxanthin; Lut-lutein; Chlc2-MGDG1-chlorophyll c_2-monogalactosyldiacylglyceride ester [18:4/14:0]; Chlc2-MGDG2- chlorophyll c_2-monogalactosyldiacylglyceride ester [14:0/14:0].

Group	Chla	Chlb	Mg DVP	Chlc1	Chlc2	Chlc3	Per	But	Fuc	Neo	Viol	Pras	Hex	Allo	Zea	Anth	Asta	Lut	Chlc2-MG DG1	Chlc2-MG DG2
Starting Ratios																				
Diatoms-1	1	0	0	0.087	0.18	0	0	0	0.775	0	0	0	0	0	0	0	0	0	0	0
Diatoms-2	1	0	0	0	0.284	0.083	0	0	0.998	0	0	0	0	0	0	0	0	0	0	0
Dinoflagellates	1	0	0.006	0	0.22	0	0.56	0	0	0	0	0	0	0	0	0	0	0	0	0
Cryptophytes	1	0	0	0	0.2	0	0	0	0	0	0	0	0	0.38	0	0	0	0	0	0
Pelagophytes	1	0	0	0.01	0.275	0.23	0	0.66	0.78	0	0	0	0	0	0	0	0	0	0	0
Haptophytes	1	0	0.009	0	0.21	0.18	0	0.04	0.31	0	0	0	0.47	0	0	0	0	0	0.09	0.103
Prasinophytes-1	1	0.631	0.008	0	0	0	0	0	0	0.072	0.138	0	0	0	0.026	0.023	0	0.057	0	0
Prasinophytes-3	1	0.73	0.062	0	0	0	0	0	0	0.063	0.054	0.25	0	0	0.058	0.021	0	0.021	0	0
Chlorophytes	1	0.32	0	0	0	0	0	0	0	0.066	0.049	0	0	0	0.032	0.014	0.012	0.17	0	0
Cyanobacteria (Synechococcus)	1	0	0	0	0	0	0	0	0	0	0	0	0	0	0.64	0	0	0	0	0
May 2014																				
Diatoms-1	1	0	0	0.135	0.148	0	0	0	0.761	0	0	0	0	0	0	0	0	0	0	0
Diatoms-2	1	0	0	0	0.222	0.133	0	0	0.482	0	0	0	0	0	0	0	0	0	0	0
Dinoflagellates	1	0	0.005	0	0.212	0	0.776	0	0	0	0	0	0	0	0	0	0	0	0	0
Cryptophytes	1	0	0	0	0.187	0	0	0	0	0	0	0	0	0.257	0	0	0	0	0	0
Pelagophytes	1	0	0	0.008	0.236	0.241	0	0.840	0.759	0	0	0	0	0	0	0	0	0	0	0
Haptophytes	1	0	0.007	0	0.189	0.188	0	0.034	0.357	0	0	0	0.630	0	0	0	0	0	0.061	0.066
Prasinophytes-1	1	0.427	0.008	0	0	0	0	0	0	0.060	0.153	0	0	0	0.018	0.023	0	0.055	0	0
Prasinophytes-3	1	0.980	0.082	0	0	0	0	0	0	0.060	0.069	0.120	0	0	0.076	0.026	0	0.017	0	0
Chlorophytes	1	0	0	0	0	0	0	0	0	0	0	0	0	0	0	0	0	0	0	0
Cyanobacteria (Synechococcus)	1	0	0	0	0	0	0	0	0	0	0	0	0	0	0.832	0	0	0	0	0
September 2014																				
Diatoms-1	1	0	0	0.088	0.101	0	0	0	0.513	0	0	0	0	0	0	0	0	0	0	0
Diatoms-2	1	0	0	0	0.258	0.109	0	0	0.851	0	0	0	0	0	0	0	0	0	0	0
Dinoflagellates	1	0	0.008	0	0.154	0	0.742	0	0	0	0	0	0	0	0	0	0	0	0	0
Cryptophytes	1	0	0	0	0.168	0	0	0	0	0	0	0	0	0.368	0	0	0	0	0	0
Pelagophytes	1	0	0	0.008	0.194	0.293	0	0.763	0.819	0	0	0	0	0	0	0	0	0	0	0
Haptophytes	1	0	0.012	0	0.323	0.299	0	0.042	0.397	0	0	0	0.793	0	0	0	0	0	0.133	0.129
Prasinophytes-1	1	0.601	0.008	0	0	0	0	0	0	0.063	0.096	0	0	0	0.028	0.029	0	0.045	0	0
Prasinophytes-3	1	0.687	0.069	0	0	0	0	0	0	0.064	0.054	0.129	0	0	0.056	0.018	0	0.014	0	0
Chlorophytes	1	0.315	0	0	0	0	0	0	0	0.088	0.046	0	0	0	0.042	0.019	0.015	0.215	0	0
Cyanobacteria (Synechococcus)	1	0	0	0	0	0	0	0	0	0	0	0	0	0	0.642	0	0	0	0	0

Table 2

Dominant diatom and dinoflagellate species at the surface for each station on the 20°S and 23°S transects during May and September 2014. *Pseudo-nitzschia* seriata-gr indicates *Pseudo-nitzschia* seriata-group. *Pseudo-nitzschia* delicatissima-gr indicates *Pseudo-nitzschia* delicatissima-group.

May	Diatoms	Cells L^{-1}	Dinoflagellates	Cells L^{-1}	September	Diatoms	Cells L^{-1}	Dinoflagellates	Cells L^{-1}
20°S	*Pseudo-nitzschia* seriata-gr	$14.89x10^3$	*Ceratium* spp	$5.47x10^3$	20°S	*Thalassiosira gravida*	$21.33x10^4$	*Gyrodinium* spp	$4.35x10^3$
2	*Chaetoceros curvisetus*	$11.45x10^3$	*Prorocentrum micans*	$4.58x10^3$	2				
			Unidentified dinoflagellates	$3.43x10^3$					
					20°S	*Thalassiosira gravida*	$84.45x10^4$	*Gymnodenium* spp	$7.33x10^3$
					5	*Pseudo-nitzschia* seriata-gr	$22.63x10^4$	*Gyrodinium* spp	$6.18x10^3$
								Protoperidinium spp	$5.38x10^3$
20°S	*Chaetoceros curvisetus*	$13.40x10^4$	*Ceratium* spp	$14.04x10^3$	20°S	*Thalassiosira gravida*	$77.92x10^4$	*Gyrodinium* spp	$28.98x10^3$
10	*Pseudo-nitzschia* seriata-gr	$66.44x10^3$			10	*Thalassiosira rotula*	$28.73x10^4$	*Scrippsiella trochoidea*	$10.88x10^3$
								Noctiluca scintillans	$10.31x10^3$
20°S	*Chaetoceros debilis*	$24.51x10^4$	*Ceratium* spp	$42.92x10^3$	20°S	*Thalassiosira rotula*	$82.71x10^3$	Unidentified dinoflagellates	$4.12x10^3$
20	*Pseudo-nitzschia* seriata-gr	$24.40x10^4$			20	*Leptocylindrus danicus*	$60.94x10^3$		
	Chaetoceros curvisetus	$10.65x10^4$							
20°S	*Pseudo-nitzschia* seriata-gr	$2.67x10^6$	Unidentified dinoflagellates	$9.16x10^3$	20°S	*Leptocylindrus danicus*	$32.21x10^4$	*Ceratium furca*	$10.66x10^3$
30	*Chaetoceros curvisetus*	$2.08x10^6$			30	*Thalassiosira gravida*	$28.73x10^4$	Unidentified dinoflagellates	$6.53x10^3$
	Chaetoceros debilis	$1.39x10^6$				*Thalassiosira anguste-lineata*	$27.64x10^4$	*Dinophysis fortii*	$6.30x10^3$
20°S	*Thalassiosira gravida*	$69.42x10^4$	*Corythodinium tesselatus*	$1.14x10^3$	20°S	*Pseudo-nitzschia* seriata-gr	$76.18x10^3$	Unidentified dinoflagellates	$30.24x10^3$
40	*Bacteriastrum delicatulum*	$35.17x10^4$	*Gyrodinium* spp	$1.14x10^3$	40	*Leptocylindrus danicus*	$74.01x10^3$	*Prorocentrum triestinum*	$23.94x10^3$
						Thalassiosira gravida	$39.18x10^3$		
20°S	*Bacteriastrum delicatulum*	$1.62x10^6$	Unidentified dinoflagellates	$8.02x10^3$	20°S	*Thalassiosira gravida*	$10.40x10^4$	Unidentified dinoflagellates	$4.12x10^3$
50	*Pseudo-nitzschia* seriata-gr	$88.44x10^4$	*Protoperidinium pallidum*	$3.43x10^3$	50	*Leptocylindrus danicus*	$85.57x10^3$		
20°S	*Bacteriastrum hyalinum*	$97.15x10^4$	*Protoperidinium* spp	$2.29x10^3$	20°S	*Thalassiosira gravida*	$78.36x10^3$	*Scrippsiella trochoidea*	$9.28x10^3$
60					60	*Chaetoceros decipiens*	$53.61x10^3$	*Dinophysis acuminata*	$6.18x10^3$
						Chaetoceros didymus	$53.61x10^3$	Unidentified dinoflagellates	$6.18x10^3$
20°S	*Bacteriastrum delicatulum*	$2.16x10^6$	Unidentified dinoflagellates	$2.29x10^3$	20°S	*Thalassiosira gravida*	$14.43x10^3$	Unidentified dinoflagellates	$11.34x10^3$
70					70			*Prorocentrum triestinum*	$8.25x10^3$
23°S	*Cylindrotheca closterium*	$36.66x10^4$	Naked dinoflagellates	$12.60x10^3$	23°S	*Skeletonema japonica*	$20.62x10^3$	*Prorocentrum triestinum*	$1.14x10^3$
2			*Prorocentrum micans*	$5.72x10^3$	2	*Navicula* spp	$12.60x10^3$		
23°S	*Cylindrotheca closterium*	$73.32x10^3$	Unidentified dinoflagellates	$10.31x10^3$	23°S	Unidentified diatoms	$2.29x10^3$	*Protoperidinium* spp	$1.14x10^3$
5	*Pseudo-nitzschia* seriata-gr	$37.81x10^3$	*Protoperidinium* spp	$5.72x10^3$	5				
	Bacteriastrum hyalinum	$29.78x10^3$							
23°S	*Pseudo-nitzschia* seriata-gr	$82.48x10^3$	Naked dinoflagellates	$17.18x10^3$	23°S	*Pseudo-nitzschia* delicatissima-gr	$3.43x10^3$	Unidentified dinoflagellates	$1.14x10^3$
10			Unidentified dinoflagellates	$13.74x10^3$	10	*Navicula* spp	$2.29x10^3$		
23°S	*Pseudo-nitzschia* seriata-gr	$12.48x10^4$	Unidentified dinoflagellates	$6.87x10^3$	23°S	*Chaetoceros curvisetus*	$73.32x10^3$	*Dinophysis fortii*	$1.14x10^3$
20					20			*Protoperidinium* spp	$1.14x10^3$
23°S	*Pseudo-nitzschia* seriata-gr	$12.71x10^4$	Unidentified dinoflagellates	$8.02x10^3$	23°S	*Chaetoceros constrictus*	$6.87x10^3$	*Scrippsiella trochoidea*	$4.58x10^3$
30			*Ceratium* spp	$3.37x10^3$	30				
23°S	*Pseudo-nitzschia* seriata-gr	$3.83x10^6$	Naked dinoflagellates	$4.58x10^3$	23°S	*Chaetoceros curvisetus*	$1.14x10^3$	Unidentified dinoflagellates	$2.29x10^3$
40			*Scrippsiella trochoidea*	$3.43x10^3$	40				
23°S	*Rhizosolenia robusta*	$1.05x10^3$	Unidentified dinoflagellates	$5.72x10^3$	23°S	*Chaetoceros convolutus*	$14.89x10^3$	None	
50	*Cylindrotheca closterium*	$1.14x10^3$			50				

	Centric diatoms	$1.14x10^3$							
23^oS	Centric diatoms	$8.02x10^3$	*Scrippsiella trochoidea*	$13.74x10^3$	23^oS	*Pseudo-nitzschia* delicatissima-gr	$32.07x10^3$	*Gyrodinium* spp	$2.29x10^3$
60	*Pseudo-nitzschia* seriata-gr	$5.72x10^3$	*Gyrodinium* spp	$5.72x10^3$	60	*Chaetoceros atlanticus*	$22.91x10^3$		
						Pseudo-nitzschia seriata-gr	$20.62x10^3$		
23^oS	*Thalassiosira* sp	$12.94x10^4$	Naked dinoflagellates	$5.72x10^3$	23^oS	*Pseudo-nitzschia* delicatissima-gr	$67.59x10^3$	Unidentified dinoflagellates	$3.43x10^3$
70					70			*Protoperidinium oblongum*	$1.14x10^3$

682
683

Figure legends

Figure 1. Monthly composites of MODIS Aqua Sea Surface Temperature for (a) May 2014 and (c) September 2014, and chlorophyll *a* concentration for (b) May 2014 and (d) September 2014. Black dots and squares indicate positions of sampling stations on the 20°S and 23°S transects and the ZZ stations respectively. White areas indicate missing data due to cloud cover or fog. Abbreviations are WB-Walvis Bay, SW-Swakopmund, CC-Cape Cross, TC-Toscanini, TB-Terrace Bay. The images provide a larger "aerial view" geographic and hydrographic context for the two cruise periods.

Figure 2. Daily Eckman transport (dark grey) for 6-18 May 2014 at (a) 20°S and (b) 23°S and for 5-16 September 2014 at (c) 20°S and (d) 23°S. Light grey indicates the cruise periods for 9-15 May and 8-13 September 2014.

Figure 3. Temperature profiles on the 20°S transect for (a) May 2014 and (c) September 2014, and on the 23°S transect for (b) May 2014 and (d) September 2014. Horizontal black lines indicate the depth of the upper mixed layer (Z_m). Vertical dotted lines indicate the depth of CTD profiles.

Figure 4. Salinity profiles on the 20°S transect for (a) May 2014 and (c) September 2014, and on the 23°S transect for (b) May 2014 and (d) September 2014. Horizontal black lines indicate the depth of the upper mixed layer (Z_m). Vertical dotted lines indicate the depth of CTD profiles.

Figure 5. Temperature profiles on the ZZ inshore transect for (a) May 2014 and (c) September 2014, and on the ZZ offshore transect for (b) May 2014 and (d) September 2014. Horizontal black lines indicate the depth of the upper mixed layer (Z_m). Vertical dotted lines indicate the depth of CTD profiles.

Figure 6. Surface pattern on the 20°S transect during May and September 2014 for (a, d) temperature and nutrients, (b, e) TChla, and (c, f) the proportion of each phytoplankton group contributing to TChla.

Figure 7. Surface pattern on the 23°S transect during May and September 2014 for (a, d) temperature and nutrients, (b, e) TChla, and (c, f) the proportion of each phytoplankton group contributing to TChla.

Figure 8. Surface pattern at the ZZ inshore stations during May and September 2014 for (a, d) temperature, (b, e) TChla, and (c, f) the proportion of each phytoplankton group contributing to TChla.

Figure 9. Surface pattern at the ZZ offshore stations during May and September 2014 for (a, d) temperature, (b, e) TChla, and (c, f) the proportion of each phytoplankton group contributing to TChla.

Fig. 1

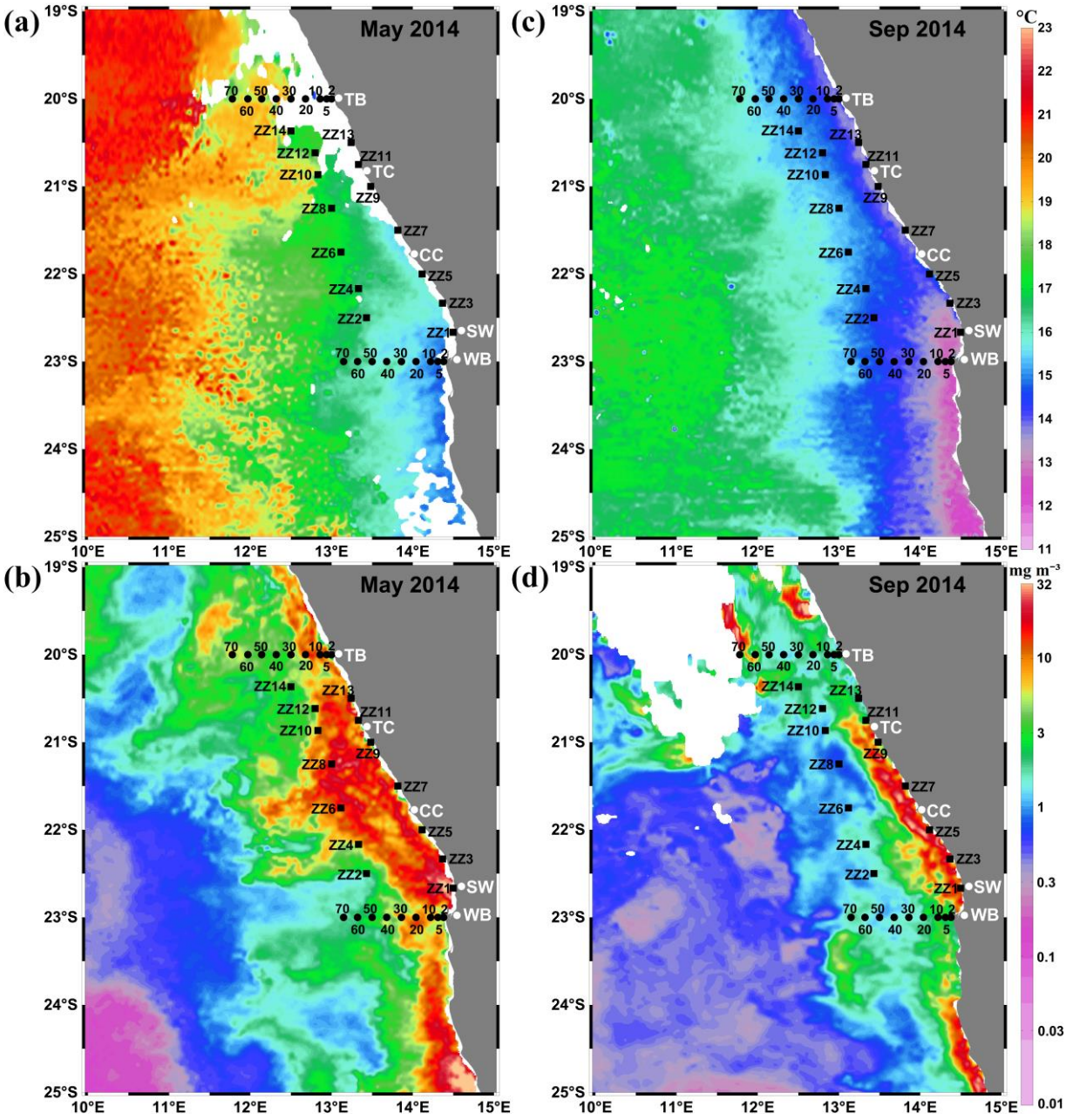
(a)
May 2014
(c)
Sep 2014
(b)
May 2014
(d)
Sep 2014
°C
mg m⁻³
TB
TC
CC
SW
WB
ZZ1
ZZ2
ZZ3
ZZ4
ZZ5
ZZ6
ZZ7
ZZ8
ZZ9
ZZ10
ZZ11
ZZ12
ZZ13
ZZ14
19°S
20°S
21°S
22°S
23°S
24°S
25°S
10°E
11°E
12°E
13°E
14°E
15°E

Fig. 2

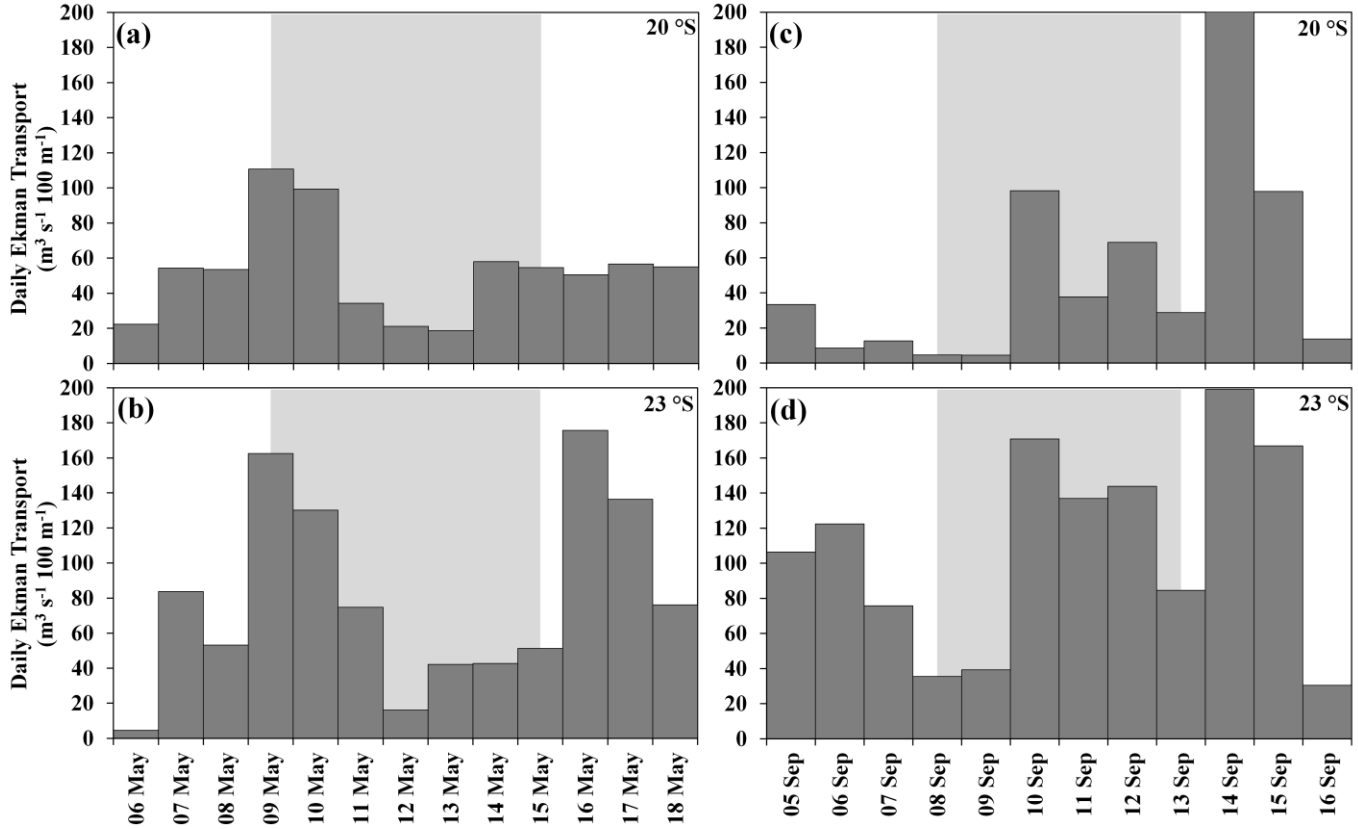
(a)
20 °S
(b)
23 °S
(c)
20 °S
(d)
23 °S
Daily Ekman Transport
(m³ s⁻¹ 100 m⁻¹)
06 May
07 May
08 May
09 May
10 May
11 May
12 May
13 May
14 May
15 May
16 May
17 May
18 May
05 Sep
06 Sep
07 Sep
08 Sep
09 Sep
10 Sep
11 Sep
12 Sep
13 Sep
14 Sep
15 Sep
16 Sep

Fig. 3

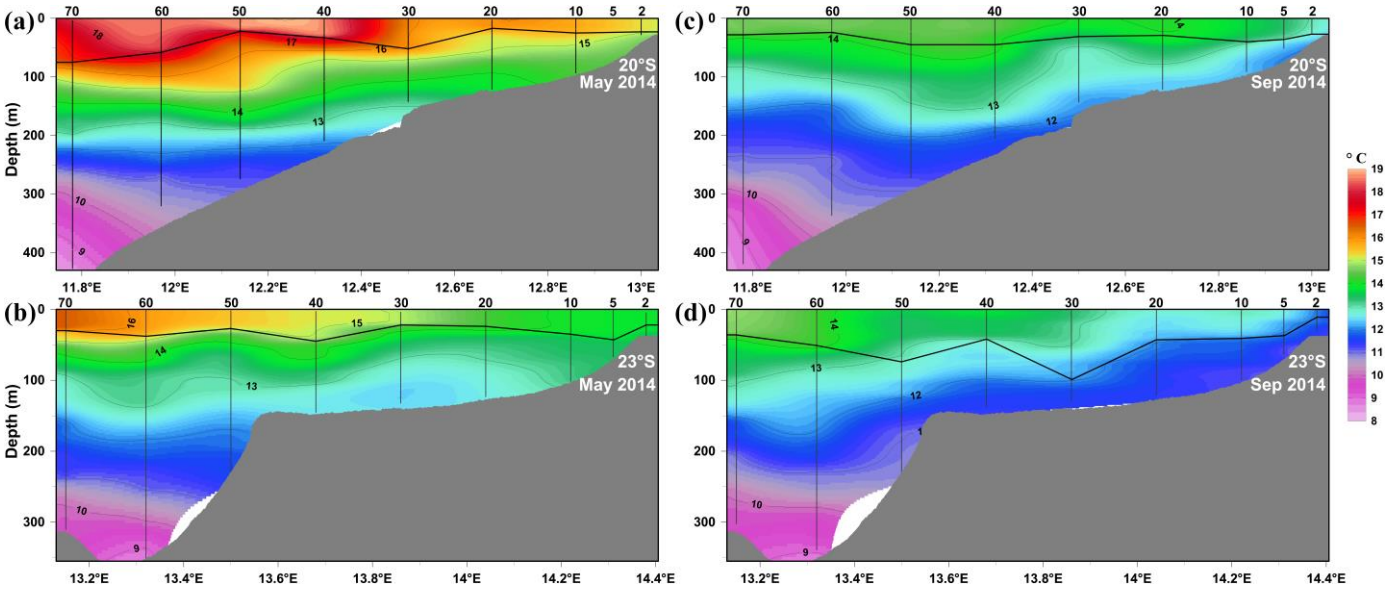
(a)
20°S
May 2014
(b)
23°S
May 2014
(c)
20°S
Sep 2014
(d)
23°S
Sep 2014
Depth (m)
°C

Fig. 4

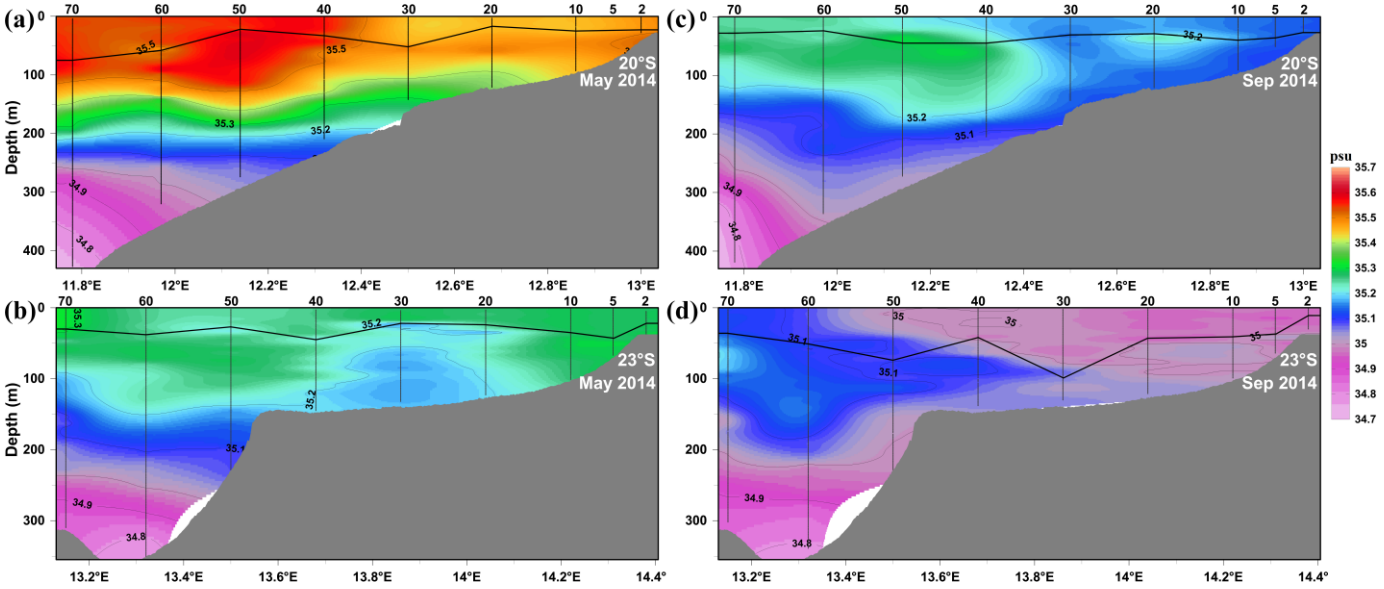
(a)
(b)
(c)
(d)
Depth (m)
20°S
May 2014
23°S
May 2014
20°S
Sep 2014
23°S
Sep 2014
psu
35.7
35.6
35.5
35.4
35.3
35.2
35.1
35
34.9
34.8
34.7

Fig. 5

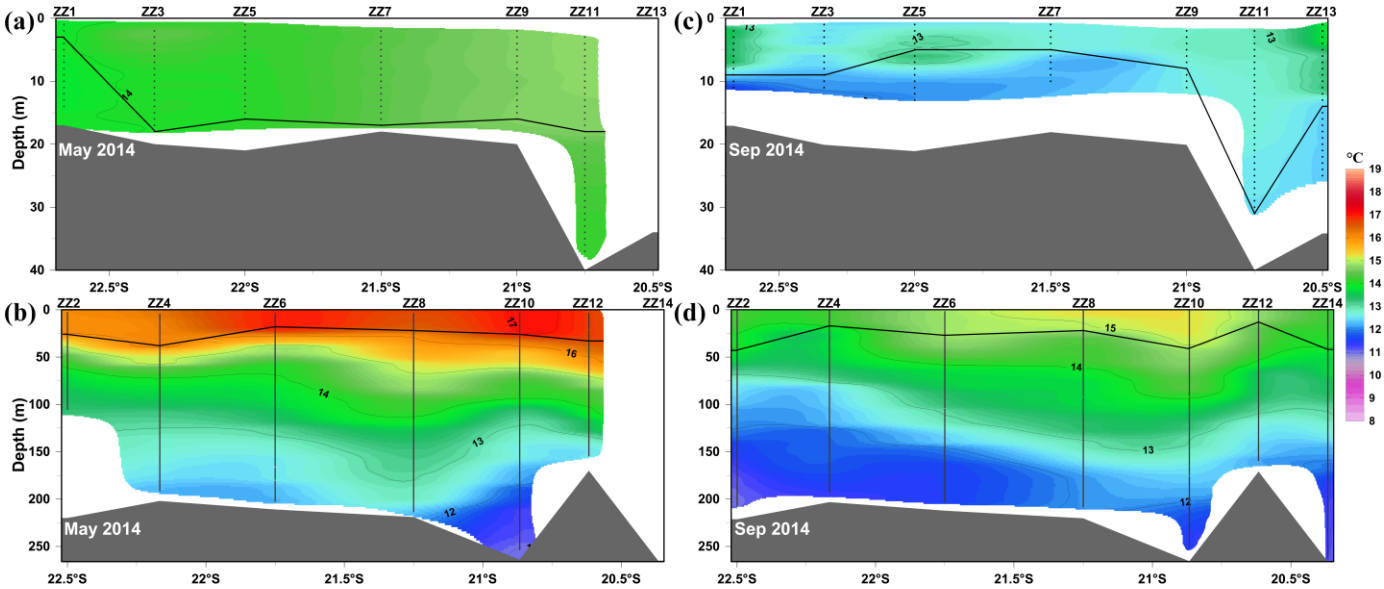
(a)
(b)
(c)
(d)
Depth (m)
May 2014
May 2014
Sep 2014
Sep 2014
°C
19
18
17
16
15
14
13
12
11
10
9
8

Fig. 6

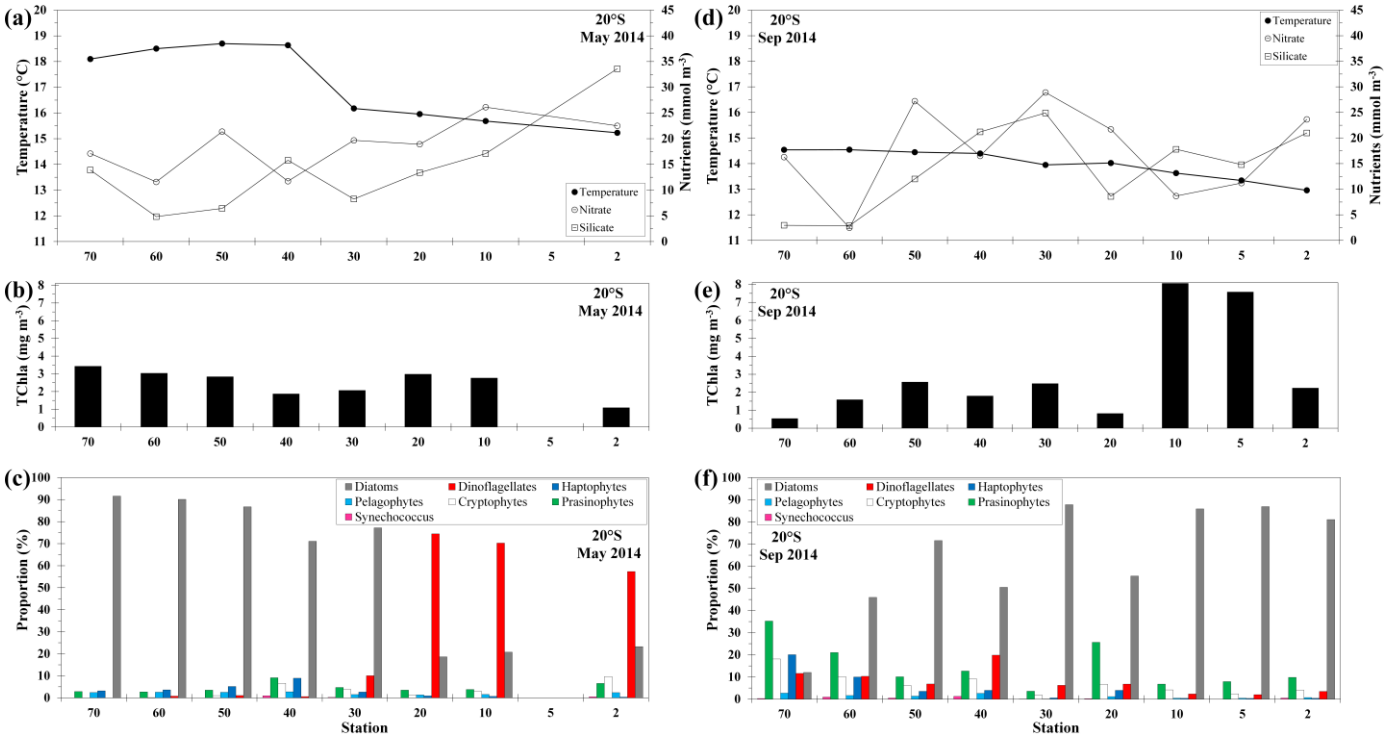
(a)
20°S
May 2014
Temperature (°C)
Nutrients (mmol m-3)
Temperature
Nitrate
Silicate
(d)
20°S
Sep 2014
(b)
TChla (mg m-3)
(e)
(c)
Proportion (%)
Diatoms
Dinoflagellates
Haptophytes
Pelagophytes
Cryptophytes
Prasinophytes
Synechococcus
(f)
Station

Fig. 7

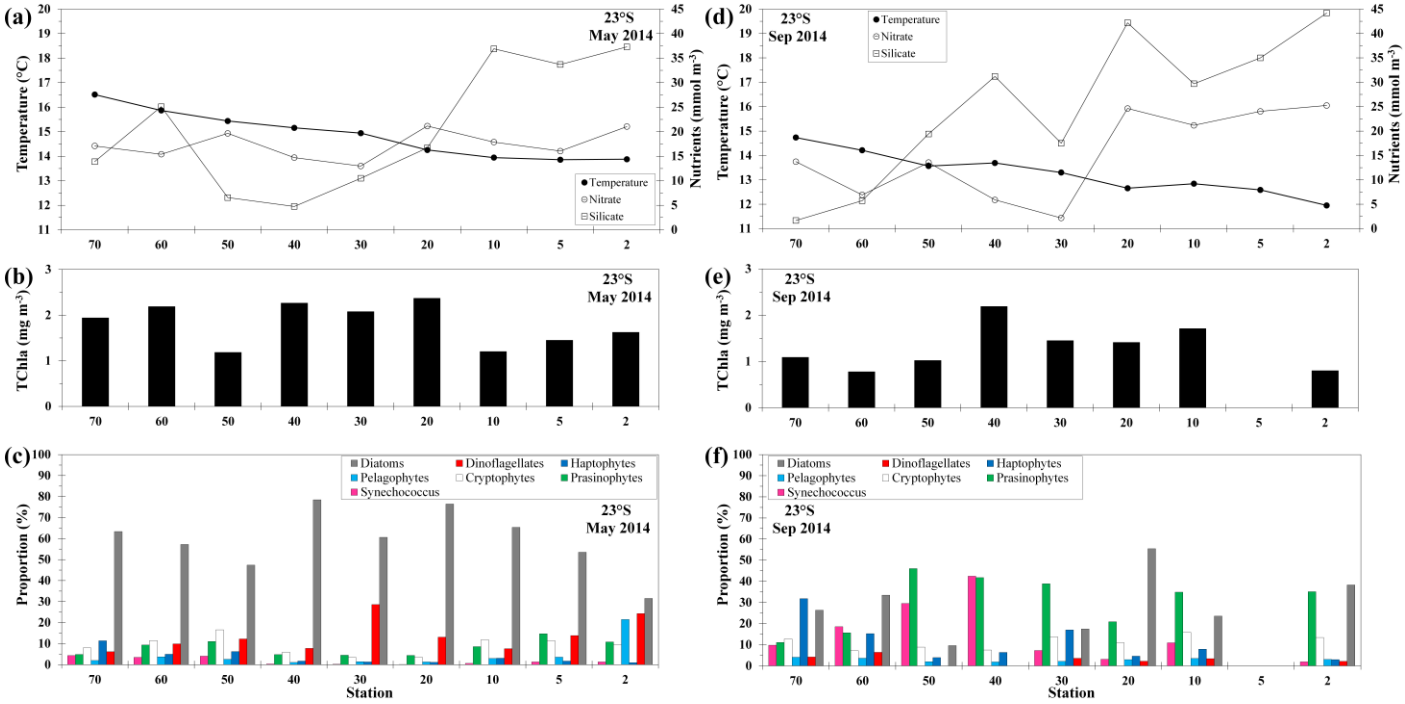
(a)
23°S
May 2014
Temperature (°C)
Nutrients (mmol m-3)
Temperature
Nitrate
Silicate
(d)
23°S
Sep 2014
(b)
TChla (mg m-3)
(e)
(c)
Proportion (%)
Diatoms
Dinoflagellates
Haptophytes
Pelagophytes
Cryptophytes
Prasinophytes
Synechococcus
(f)
Station

Fig. 8

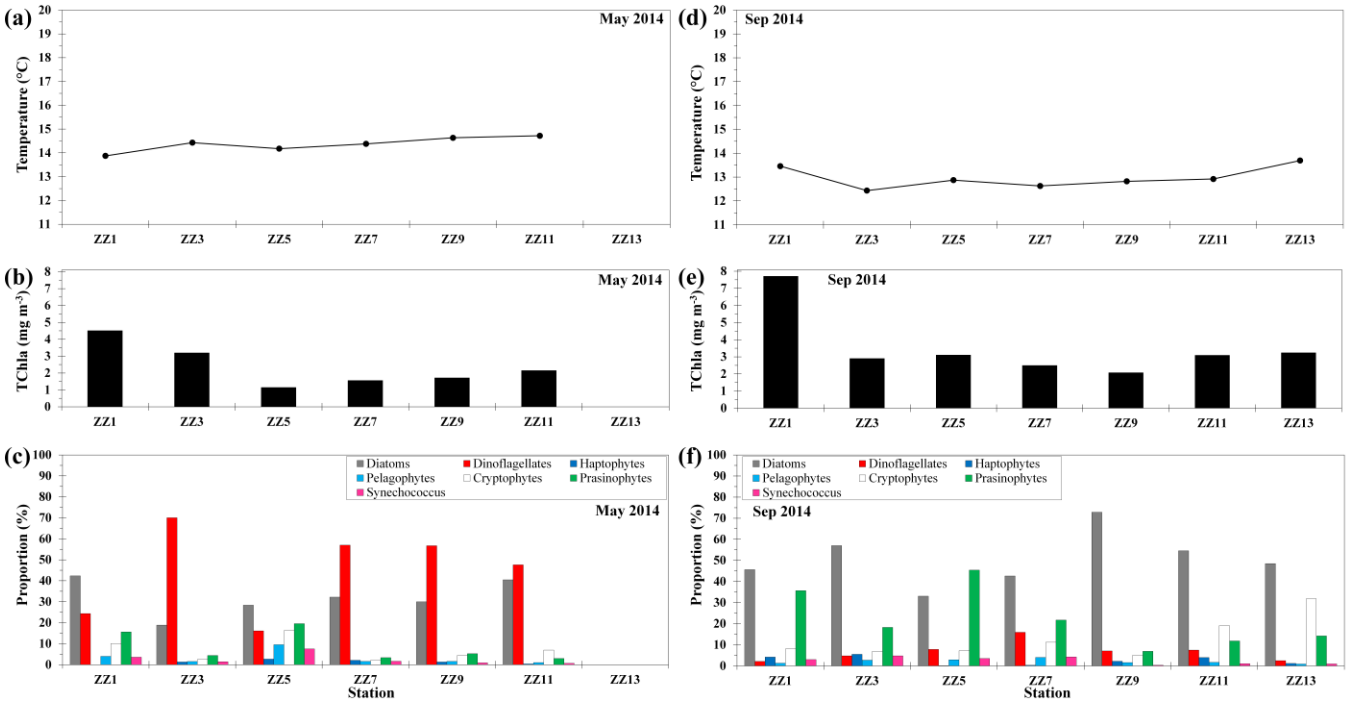
(a)
May 2014
Temperature (°C)
(d)
Sep 2014
Temperature (°C)
(b)
May 2014
TChla (mg m-3)
(e)
Sep 2014
TChla (mg m-3)
(c)
Diatoms
Dinoflagellates
Haptophytes
Pelagophytes
Cryptophytes
Prasinophytes
Synechococcus
May 2014
Proportion (%)
(f)
Sep 2014
Proportion (%)
ZZ1
ZZ3
ZZ5
ZZ7
ZZ9
ZZ11
ZZ13
Station

Fig. 9

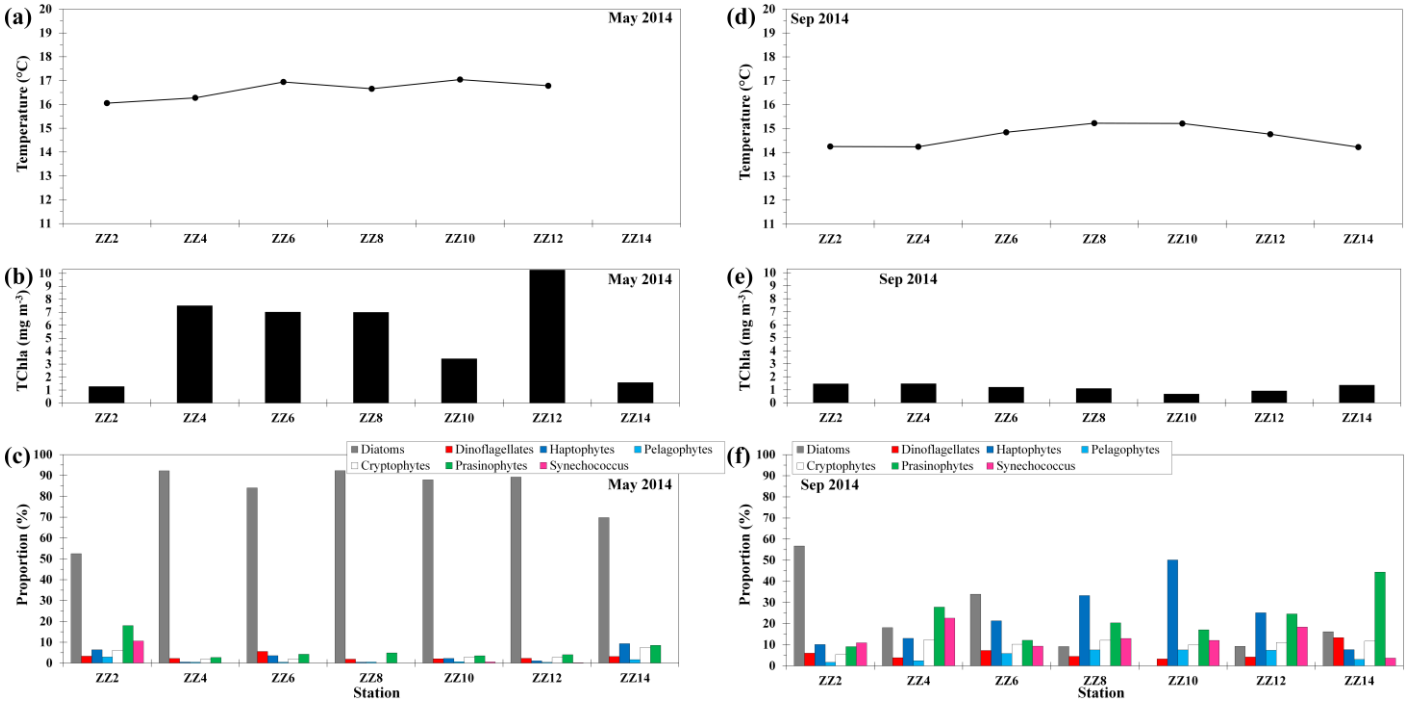
(a)
May 2014
Temperature (°C)
(d)
Sep 2014
Temperature (°C)
(b)
May 2014
TChla (mg m-3)
(e)
Sep 2014
TChla (mg m-3)
(c)
Diatoms
Dinoflagellates
Haptophytes
Pelagophytes
Cryptophytes
Prasinophytes
Synechococcus
May 2014
Proportion (%)
(f)
Sep 2014
Proportion (%)
ZZ2
ZZ4
ZZ6
ZZ8
ZZ10
ZZ12
ZZ14
Station